Constitutive modelling of soft biological tissue from ex vivo to in vivo: myocardium as an example

Debao Guan, Xiaoyu Luo and Hao Gao

Abstract Imbalance of stress/strain microenvironment can lead to adverse remodelling and pathogenesis in various soft tissues, tumour included. Therefore, there is a critical need for accurate quantification of the biomechanical homeostasis in soft tissue through mathematical modelling, which is critically dependent on constitutive models, the mathematical descriptions that approximate the mechanical behaviours of material under specific conditions by considering information from subcellular, cellular and tissue levels. In most soft biological tissue, collagen is the major component of the extracellular matrix, its architecture largely determines the material property (stiffness). In this work, we will use myocardium as an example to show how we can develop a constitutive law from various ex vivo experiments within the continuum mechanics framework, and demonstrate the applications to real patient data. We will further focus on parameter calibrations from ex/in vivo measurements. We believe this approach of constitutive modelling and calibration can be applied to various soft biological tissues and shed light on physiological and pathological mechanobiology.

1 Introduction

Imbalance of stress/strain micro-environment can lead to adverse remodelling in various organs and further causing functional deterioration. For example, imbalance

Debao Guan
School of Mathematics and Statistics, University of Glasgow e-mail: d.guan.1@research.gla.ac.uk

Xiaoyu Luo
School of Mathematics and Statistics, University of Glasgow e-mail: xiaoyu.luo@glasgow.ac.uk

Hao Gao
School of Mathematics and Statistics, University of Glasgow e-mail: hao.gao@glasgow.ac.uk

of stress/strain can regulate tumour immunity and even promote metastasis [6]. The kinematics of soft tissue can be quantitatively measured by various experimental techniques [4, 20, 17]. However, direct measurements of in vivo solid stress have not been achieved, and still challenging in in vivo situation. To overcome this difficulty, a common way is to compute stresses by using constitutive models which characterize the relation between kinematics and stresses. In this respect, there is a critical need for accurate quantification of the biomechanical micro-environment in soft tissue through mathematical modelling, which is essentially dependent on constitutive models. Constitutive models are mathematical descriptions that approximate the mechanical behaviours of material under specific conditions, which can further take into account information from different scales [12]. In most soft biological tissue, collagen is the major component of the extracellular matrix, and largely determines the material property (stiffness), cancerous tissue included [6].

In this study, we will use myocardium as an example to show how we can develop a constitutive law from various ex vivo experiments, and further show the applications to real patient data by encompassing a wide range of cross-scale soft tissue mathematical models. In the past several decades, a few constitutive models have been proposed for myocardium [12]. Myocardium is usually treated as an anisotropic, hyper-elastic material with layered collagen network [8, 10, 11]. One of very widely used model is the Holzapfel and Ogden (HO) model and its variations [12]. To account for fine structures of collagen fibres, general structural tensors were further introduced to describe fibre dispersion by Eriksson et al.[5]. Calibrating unknown parameters in the HO model has been investigated in [10] using three different sets of ex vivo experiment data, and inverse estimation of its unknown parameters from in vivo data was first reported in [8] by using magnetic resonance imaging.

2 Constitutive modelling of soft biological tissue

In this section, we will briefly introduce the essential continuum mechanics for soft tissue mechanics. Consider a soft tissue under certain external loading, and the material point $\mathbf{X}$ in the reference configuration will move to a new position $\mathbf{x} = \mathbf{x}(\mathbf{X}, t)$ at time t. The deformation gradient associated with the soft tissue is defined as $\mathbf{F} = \partial\mathbf{x}/\partial\mathbf{X}$, the shape change in 3-dimension. By assuming the soft tissue is hyperelastic and incompressible, then there exists a constitutive law $\mathcal{W}$, and the Cauchy stress is $\boldsymbol{\sigma} = \mathbf{F}\frac{\partial\mathcal{W}}{\partial\mathbf{F}} - p\mathbf{I}$, where the Lagrange multiplier p enforces incompressibility and $\mathbf{I}$ is the identity tensor. In addition, associated with $\mathbf{F}$ are the left and right Cauchy-Green tensors, they are $\mathbf{B} = \mathbf{F}\mathbf{F}^T$ and $\mathbf{C} = \mathbf{F}^T\mathbf{F}$, respectively, and the Green-Lagrange strain tensor is $\mathbf{E} = (\mathbf{C} - \mathbf{I})/2$.

Invariants of the right Cauchy–Green deformation tensor $\mathbf{C}$ are commonly used in formulating the strain energy function $\mathcal{W}$, likewise $I_1 = \mathrm{tr}(\mathbf{C})$, $I_2 = \frac{1}{2}\{[\mathrm{tr}(\mathbf{C})]^2 - \mathrm{tr}(\mathbf{C}^2)\}$, $I_3 = \det(\mathbf{C})$. An example is the incompressible Neo-Hooken material $W = C_1(I_1 - 3)$, in which C_1 is a material constant. Strain invariant-based constitutive

laws can be widely found for characterizing and modelling various soft tissues, such as myocardium [12] and solid cancer [23].

In order to characterize anisotropic hyperelastic myocardium, for example, to take into account the stiffening effects of the collagen network and its preferred orientation, extra strain invariants are needed. Transversely isotropic models were firstly proposed by assuming all fibres (mainly collagen) are aligned perfectly in one direction and share the same mechanical properties. Denote the fibre direction $\mathbf{f}_0$ in the reference configuration, two related strain invariants can be introduced,

$$I_{4\mathrm{f}} = \mathbf{f}_0 \cdot (\mathbf{C}\mathbf{f}_0), \qquad I_{5\mathrm{f}} = \mathbf{f}_0 \cdot (\mathbf{C}^2\mathbf{f}_0). \tag{1}$$

The strain energy function for such one family fibre can be formulated as $\mathcal{W}(I_1, I_2, I_3, I_{4\mathrm{f}}, I_{5\mathrm{f}})$ with I_1, I_2, I_3 for its isotropic response and $I_{4\mathrm{f}}, I_{5\mathrm{f}}$ for fibre contributions. In actual applications, reduced formula $\mathcal{W}(I_1, I_{4\mathrm{f}})$ is often found [11]. The corresponding Cauchy stress is

$$\boldsymbol{\sigma} = 2\frac{\partial \mathcal{W}}{\partial I_1}\mathbf{B} + 2\frac{\partial \mathcal{W}}{\partial I_{4\mathrm{f}}}\mathbf{f}\otimes\mathbf{f} - p\mathbf{I}, \quad \text{and} \quad \mathbf{f} = \mathbf{F}\mathbf{f}_0. \tag{2}$$

Experimental studies have shown that myocardium has layered myofibre structure with three families of fibres, the so-called fibre ($\mathbf{f}_0$)–sheet($\mathbf{s}_0$)–normal($\mathbf{n}_0$) system, or $f-s-n$ in short. Additional strain invariants are

$$\begin{aligned} &I_{4\mathrm{s}} = \mathbf{s}_0 \cdot (\mathbf{C}\mathbf{s}_0),\ I_{5\mathrm{s}} = \mathbf{s}_0 \cdot (\mathbf{C}^2\mathbf{s}_0),\ I_{4\mathrm{n}} = \mathbf{n}_0 \cdot (\mathbf{C}\mathbf{n}_0),\ I_{5\mathrm{n}} = \mathbf{n}_0 \cdot (\mathbf{C}^2\mathbf{n}_0),\\ &I_{8\mathrm{fs}} = \mathbf{f}_0 \cdot (\mathbf{C}\mathbf{s}_0),\ I_{8\mathrm{fn}} = \mathbf{f}_0 \cdot (\mathbf{C}\mathbf{n}_0),\ I_{8\mathrm{ns}} = \mathbf{n}_0 \cdot (\mathbf{C}\mathbf{s}_0). \end{aligned} \tag{3}$$

As discussed in [12], not all strain invariants are independent, thus we can omit some of these in the functional dependence of the strain energy function. Based on the simple shear data of ex vivo porcine myocardium [4], Holzapfel and Ogden proposed the micro-structure informed strain energy function for myocardium by only including I_1, $I_{4\mathrm{f}}$, $I_{4\mathrm{s}}$, $I_{8\mathrm{fs}}$ (the HO law),

$$\mathcal{W} = \frac{a}{2b}\{e^{b(I_1-3)} - 1\} + \sum_{i=\mathrm{f,s}} \frac{a_i}{2b_i}\{e^{b_i(I_{4i}-1)^2} - 1\} + \frac{a_{\mathrm{fs}}}{2b_{\mathrm{fs}}}\{e^{I_{8\mathrm{fs}}^2} - 1\}, \tag{4}$$

where a, b, a_{f}, b_{f},a_{s}, b_{s}, a_{fs} and b_{fs} are material parameters. The corresponding Cauchy stress tensor is

$$\begin{aligned} \boldsymbol{\sigma} =& a_1 e^{b_1(I_1-3)}\mathbf{B} + 2a_{\mathrm{f}}(I_{4\mathrm{f}}-1)e^{b_{\mathrm{f}}(I_{4\mathrm{f}}-1)^2}\mathbf{f}\otimes\mathbf{f}\\ &+ 2a_{\mathrm{s}}(I_{4\mathrm{s}}-1)e^{b_{\mathrm{s}}(I_{4\mathrm{s}}-1)^2}\mathbf{s}\otimes\mathbf{s} + a_{\mathrm{fs}}I_{8\mathrm{fs}}e^{I_{8\mathrm{fs}}^2}(\mathbf{f}\otimes\mathbf{s} + \mathbf{s}\otimes\mathbf{f}), \end{aligned} \tag{5}$$

in which $\mathbf{s} = \mathbf{F}\mathbf{s}_0$. Since its introduce, the HO law in Equation (4) has been widely used in characterizing myocardial mechanic behaviours in various ex vivo experiments [10] and in vivo cardiac function modelling [8].

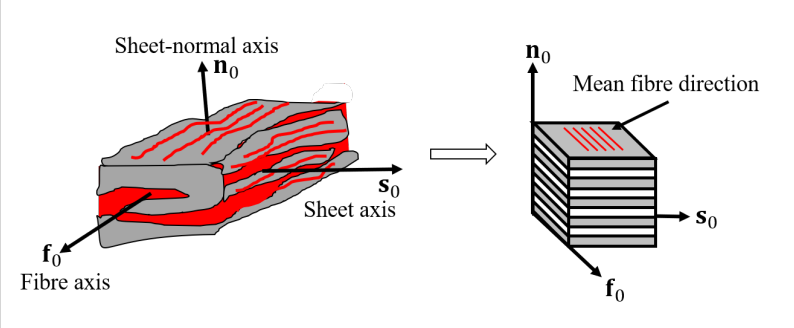

Fig. 1 The sketch of layered organization of myocytes and the collagen fibres between the sheets in the orthonormal coordinate system with fibre axis $\mathbf{f}_0$, sheet axis $\mathbf{s}_0$ and sheet-normal axis $\mathbf{n}_0$. An additional cube of layered tissue serving as the base for the constitutive model in the simulation. (Figure is cited from Holzapfel & Ogden [12])

3 Ex vivo calibration

Experimental tests of passive properties of the myocardium are usually performed on tissue level at ex vivo condition because of easy setup and operation compared to the experiments on the cellular level [4, 20]. By assuming the experimental specimen to be homogeneous, measured stresses and strains can be used to inform the underlying formulations of constitutive behaviours. For example, simple shear tests have been found necessary for characterizing the orthotropic nonlinear behaviours of the myocardium [4], recently extended to the combination with bi-axial tests [20], and further demonstrated in [10].

In this study, we choose the simple shear experimental data from Dokos et al. [4] for inferring material constants in Eq.(4). Dokos et al firstly reported ex vivo simple shear tests on passive myocardium from porcine hearts with six different shear modes, shown in Fig. 2(a) where (ij) refers to shearing in the j direction within the ij plane, where $i \neq j \in \{\mathrm{f}, \mathrm{s}, \mathrm{n}\}$. Details of the experimental protocols can be found in [4].

The loading path in simple shear experiments can be quantified by deformation gradient tensors under homogeneous deformation assumption. For the six simple shear tests in Figure 2(a), we have

$$\begin{aligned}
&\text{(ns)}: \quad \mathbf{F} = \begin{bmatrix} 1 & 0 & 0 \\ 0 & 1 & 0 \\ 0 & \gamma_{\mathrm{ns}} & 1 \end{bmatrix}, \qquad \text{(fn)}: \quad \mathbf{F} = \begin{bmatrix} 1 & 0 & 0 \\ \gamma_{\mathrm{fn}} & 1 & 0 \\ 0 & 0 & 1 \end{bmatrix}, \quad \text{(sf)}: \quad \mathbf{F} = \begin{bmatrix} 1 & 0 & \gamma_{\mathrm{sf}} \\ 0 & 1 & 0 \\ 0 & 0 & 1 \end{bmatrix}, \\
&\text{(nf)}: \quad \mathbf{F} = \begin{bmatrix} 1 & \gamma_{\mathrm{nf}} & 0 \\ 0 & 1 & 0 \\ 0 & 0 & 1 \end{bmatrix}, \qquad \text{(fs)}: \quad \mathbf{F} = \begin{bmatrix} 1 & 0 & 0 \\ 0 & 1 & 0 \\ \gamma_{\mathrm{fs}} & 0 & 1 \end{bmatrix}, \quad \text{(sn)}: \quad \mathbf{F} = \begin{bmatrix} 1 & 0 & 0 \\ 0 & 1 & \gamma_{\mathrm{sn}} \\ 0 & 0 & 1 \end{bmatrix}, \qquad (6)
\end{aligned}$$

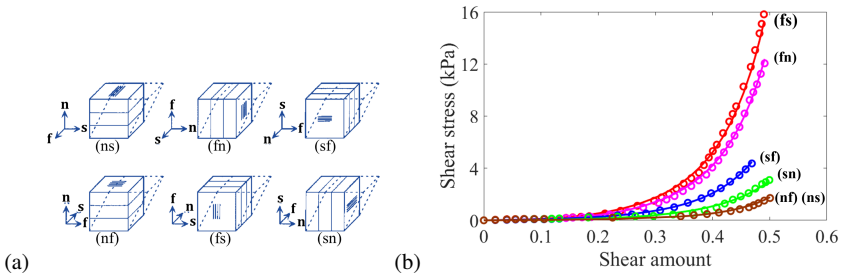

Fig. 2 Parameter inference from ex vivo experiments. (a) a sketch of all six shear modes of a cubic myocardial sample adapted from [4], **f**, **s** and **n** denote the fibre, sheet and normal direction, respectively; (b) fitted simple shear experimental data using the HO model from the optimized parameter set in Table 1.

where γ_{ij} is the shear amount with respect to the Cartesian coordinates $\{\mathbf{e}_1, \mathbf{e}_2, \mathbf{e}_3\}$, which are coincident with the local material coordinates $\{\mathbf{f}_0, \mathbf{n}_0, \mathbf{s}_0\}$. We now use the six shear experimental data [4] to inversely determine the 8 unknown parameters in Eq. (4) by using those above deformation gradients for each corresponding simple shear experiment. The inverse problem is similar as in our previous study [10] by minimising the loss function defined as the squared errors between the predicted stress from the HO law to the measured values. The goodness of fits are shown in Figure 2(b), from which we can see that the HO law is able to capture all mechanical responses of six simple shears, and the optimised parameters are listed in Table 1.

Table 1 Optimised parameters in the HO law based on the experimental data of six simple shear tests [4] and from in vivo measurements using clinical cardiac magnetic resonance imaging [9]

Parameters	a (kPa)	b	a_f (kPa)	b_f	a_s (kPa)	b_s	a_fs (kPa)	b_fs
ex vivo	0.2362	10.81	20.037	14.154	3.7245	5.1645	0.4109	11.3
in vivo	0.1	2.49	1.99456	4.92	0.243	1.188	0.1	2.6

4 Move to in vivo

To estimate myocardial passive stiffness from in vivo data is still very challenging, there is no established approach on how to adjust parameters derived from ex vivo experiments directly to in vivo situations. Studies have found that the passive stiffness estimated from ex vivo experiments will over-estimate in vivo stiffness, thus not suitable for personalized modelling. For this reason, a few studies have tried to re-scale ex vivo experimental data to match measured in vivo dynamics. In this section, an in vivo human left ventricular (LV) model reconstructed from cardiac magnetic resonance (CMR) imaging from our previous studies [9] is used as shown

in Figure 3(a) superimposed with a CMR image. The LV geometry is reconstructed at early-diastole when the LV pressure is at the lowest.

We previously proposed a three-step algorithm [8] to inversely infer the 8 constitutive parameters by matching the simulated LV dynamics at diastole to in vivo measured LV motion (the cavity volume and 24 segmental strains). To simulate the LV passive filling at diastole, a quasi-static biomechanical model is developed using the finite-element discretization and solved by ABAQUS. The boundary value problem of the LV passive filling is

$$\left.\begin{array}{ll} \nabla \cdot \boldsymbol{\sigma} + \mathbf{b} = 0 & \text{in } \Omega \\ \boldsymbol{\sigma} \cdot \mathbf{n} = \mathbf{t} & \text{in } \Gamma^{\mathrm{N}} \\ \mathbf{u} = \mathbf{u}_0 & \text{in } \Gamma^{\mathrm{D}} \end{array}\right\}, \tag{7}$$

where Ω is the LV computational domain, $\boldsymbol{\sigma}$ is Cauchy stress of Eq. (5), $\mathbf{n}$ denotes the normal direction of $\partial\Omega$, $\mathbf{b}$ is the body force density per unit volume, which is zero in this study, $\mathbf{t}$ is the traction force resulted from the LV cavity pressure, Γ^{D} is the basal plane with prescribed displacements $\mathbf{u}_0$, and Γ^{N} is the endocardial surface with linearly ramped pressure from 0 mmHg to 8 mmHg at end-diastole. Details of the LV biomechanical model can be found in our previous studies [8, 25].

Here, we introduce a modified version by taking into account ex vivo pressure–volume relationship reported by Klotz et al. [14] in the multi-step optimization procedure. In detail,

1. Optimise C_a, C_b by minimising f_{O1} using grid search within $[0.1, 1.0]$, following the widely used scaling approach by grouping the 8 parameters into two groups: $a^{\mathrm{group}} = \{a, a_{\mathrm{f}}, a_{\mathrm{s}}, a_{\mathrm{fs}}\}$, $b^{\mathrm{group}} = \{b, b_{\mathrm{f}}, b_{\mathrm{s}}, b_{\mathrm{fs}}\}$, respectively. C_a and C_b are scaling parameters as
$$a^{\mathrm{group}} = C_a a_0^{\mathrm{group}} \quad \text{and} \quad b^{\mathrm{group}} = C_b b_0^{\mathrm{group}},$$
in which a_0^{group} and b_0^{group} are from ex vivo data (see section 3). The objective function is defined as
$$f_{\mathrm{O1}} = (V^{\text{simulated}} - V^{\text{in vivo}})^2 + \sum_{i=1}^{24} (\epsilon_i^{\text{simulated}} - \epsilon^{\text{in vivo}})^2,$$
in which V is the LV cavity volume, and ϵ is the myocardial strains.
2. Refine C_a, C_b by minimising $f_{\mathrm{O1}}^{\mathrm{Klotz}}$, which is defined as
$$f_{\mathrm{O1}}^{\mathrm{Klotz}} = \Big(\frac{V_8^{\text{simulate}} - V_8}{V_8}\Big)^2 + \Big(\frac{V_{30}^{\text{simulate}} - V_{30}}{V_{30}}\Big)^2 + \sum_{i=1}^{N} (\epsilon_i^{\text{simulated}} - \epsilon^{\text{in vivo}})^2,$$
where V_8 and V_{30} are the LV cavity volumes at 8 mmHg and 30 mmHg derived from the Klotz relationship [14].
3. Optimise a_{f}, b_{f} by minimising f_{O2}, which is similar as $f_{\mathrm{O1}}^{\mathrm{Klotz}}$ by excluding the term $\big((V_{30}^{\text{simulate}} - V_{30})/V_{30}\big)^2$.

Note steps 2 and 3 use the MATLAB function *fmincon* for finding the best parameters. Details of this multistep optimization procedure can be found in [8] and its application in [9]. Figure 3 (b) compares the strains from ex vivo parameters and from the optimal set of parameters to the in vivo measured values. As pointed out in other studies [8], ex vivo parameters lead to a very stiff myocardium which has a much small strain magnitude at end-diastole, and away from the measurements (Figure 3 (b)). The optimized parameters from this in vivo heart can be found in Table 1, which is largely different from the ex vivo values.

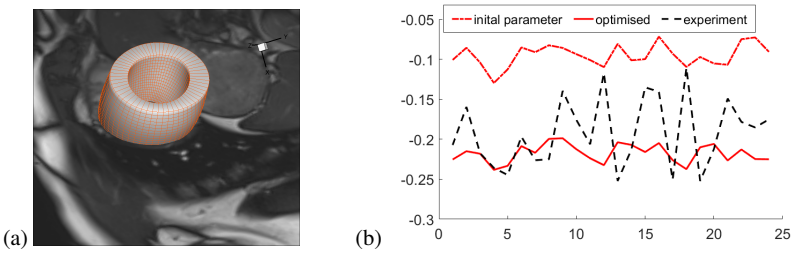

Fig. 3 Parameter calibration from in vivo data. (a) Fitted LV mesh according to the MR cine image; (b) Comparisons of regional circumferential strain at end of diastole after each optimization step.

We further compare the mechanical responses between in vivo and ex vivo parameters from Table 1 using a virtual shear experiment by shearing a cubic sample along 6 different directions up to 0.5, as shown in Figure 4(a). Clearly, in vivo myocardium is much softer than ex vivo myocardium. We then further simulate the LV filling phase by using the optimal parameters from Table 1 using the in vivo finite-element LV model (see Figure 3 and Eq.(7)) with a pressure of 8 mmHg at end-diastole. Figure 2(b) shows the deformed LV shape at end-diastole with in vivo estimated parameters (left) and ex vivo estimated parameters (right). A much larger end-diastolic volume is achieved for the in vivo parameter set (140 mL) compared to the ex vivo parameter set (70 mL), the corresponding filling volume is 85 mL and 15 mL, respectively. Figure 4(b) is further contoured by the maximum principal Cauchy stresses at end-diastole, again the two-parameter sets give very different stress levels and patterns. This suggests cautions are needed when using ex vivo experimental data for modelling the in vivo biomechanical environment.

5 Biomechanical study to cancer

There is an increased appreciation of the biomechanical environment in determining tissue development, cell differentiation and adaptation to maintain the homeostasis in healthy tissue, and the loss of this ability to maintain the local biomechanical homeostasis, such as tumour cells, will potentially contribute to its progression [6]. As has been discussed in [21], the mechanical stress environment from both the solid

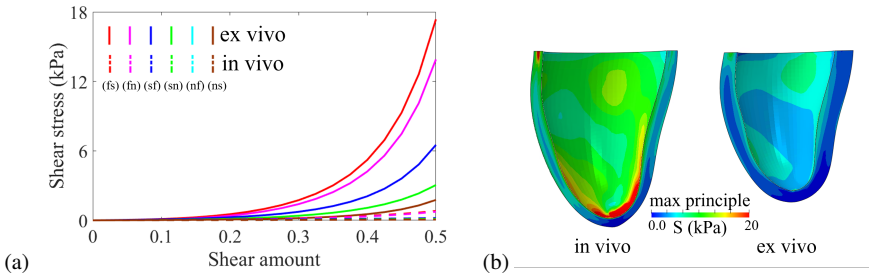

Fig. 4 Comparisons between the passive property between the ex vivo and in vivo derived parameter sets. (a) Predicted simple shear stress; (b) Simulated maximum principal stress distributions at end diastole in a human left ventricle.

and fluid phases of the tumour can play an important role in the progression and response to treatment. The elevated solid stress not only compresses intratumoral blood and lymphatic vessels, but also reduces perfusion, a major barrier to the delivery of chemotherapeutic agents and nanomedicine, causing low efficiency of those treatments. The reduced perfusion further promotes tumour progression and metastasis. Therefore, accurate quantification of solid stress in the tumour is critical for treatment planning, such as stress-reducing therapy [21]. Measuring stress is very difficult and challenging, especially in vivo, thus biomechanical predictions by solving conservations of mass, momentum, energy and entropy are usually employed along with the constitutive models of tumour tissue [23].

It is well known that solid tumour tissues are nonlinear, hierarchical and heterogeneous, thus very different from healthy tissues [19, 13]. This inherent spatially heterogeneous and hierarchical structure with its active nature make it very difficult when developing an accurate constitutive model [23]. The interplays between tumour cells and surrounding environments further complicate the accurate stress predictions. Almost over a decade ago, Unnikrishnan et al [23] reviewed the constitutive models of tumour tissue within the single-phase continuum models, the multiphase continuum models and the poroelastic models. Constitutive modelling of the myocardium presented in this study can be classified as a single phase continuum model. In this category, Chaplain and Sleeman [2] implemented a non-linear elastic material model for a growing tumour. Other constitutive laws include the incompressible neo-Hookean [15], the Blatz-Ko type model [1], etc.

Most of the aforementioned models of tumour tissue are isotropic [23], an oversimplification of the nonlinear, hierarchical heterogeneous tumour tissue. Except for tumour cells and blood and lymphatic vessels, the extracellular matrix is another major structural component with collagen being one of the most common constituents and the scaffold of tumour micro-environment, which not only behaves as a barrier to tumour cell migration, but also actively regulates tumour progression [6, 26]. Torzilli et al [22] has suggested a new paradigm in which they suggested the imbalanced biomechanical force in tumour tissue,, is the key trigger of Epithelial-mesenchymal transition, and further leads to tumour cell escaping. Therefore, it is essentially nec-

essary to take into account local collagen network into the constitutive modelling of tumour tissue with its active adaption during tumour progression. Few studies have incorporated micro-structure of collagen network in modelling biomechanics in tumour tissues. The knowledge learned from modelling soft tissue in general, will benefit the biomechanics modelling of tumour, in particular including complex collage network through fibre-reinforced models presented in this study, dispersion described by probability distributions [11, 18] and tension-compression switch [12], etc.

The procedures of inferring material constants for a selected tumour model can be obtained from ex/in vivo measurements in a similar way as presented in this study for myocardium, usually, an inverse problem is formulated. By conducting an unconfined compression experiment in tumour tissues, Voutouri et al [24] found that an exponential constitutive law can better fit the experimental data compared to widely used neo-Hookean and Blatz-Ko models. Colin et al [3] estimated the residual stress using the Ciarlet-Geymonat material model in a spherical tumour tissue combined with an in vitro incision experiment. The Ciarlet-Geymonat model describes an isotropic material consisting of four terms using the three invariants I_1, I_2 and I_3 of $\mathbf{C}$, with three material parameters. Unlike the material model used in this study, strain invariants arising from collage fibres are included for describing the anisotropic behaviours. Their parameter studies further demonstrated that with limited measurements, i.e. the opening distance of the incision, only one model parameter can be identified with confidence, and the radial stored stress could be estimated accurately. Recently, magnetic resonance elastography has been used to infer peritumoural tissue stiffness for non-invasively estimating tumour pressure through a nonlinear biomechanical model [7]. Future studies shall include different stretch modes on different types of tumour tissues at various stages and different spatial scales in order to develop competent constitutive laws, further studies shall also explore different non-invasive in vivo approaches for calibrating tumour biomechanical behaviours.

The reliability and accuracy of the biomechanical models critically depend on the model inputs, not just material properties, but also the geometry, etc. Patient-specific geometries are usually constructed by manual or semi-automatic approaches, which can have a big impact on the model predictions. While to take into account geometry uncertainty can be challenging because of its high dimension. For example, the LV geometry in this study is discretized with 133,042 nodes. The image-based geometry reconstruction procedure used in this study has recently been examined by Li et al. [16], in which an LV geometry from one patient has been reconstructed five times using the same in vivo imaging data by the same operator, and the results showed that the differences of the end-diastolic LV cavity volume and the wall volume are less than 1%. Thus, the LV geometry reconstruction procedure is highly reproducible and reliable. Interested readers refer to [9, 16] for details of image processing and geometry reconstruction. Future studies shall quantify how sensitive the geometric uncertainty affects the biomechanical environment and constitutive parameter calibration.

As discussed in [3], not all parameters can be uniquely identified from limited measured data. The identifiability issue also exists for the constitutive law used in this study, which has more parameters than the Ciarlet–Geymonat model [3]. Furthermore, parameters in the HO law is highly correlated as discussed in [8]. In our previous study [10], a repeated random initialization strategy was used for inversely estimating the parameters of the HO law using ex vivo experiments. Our results also suggest that with more measured data, more parameters can be identified. For the in vivo estimation procedure, our previous study [8] has found that even though it is very challenging to establish the uniqueness of the solution of the inverse problem because of its ill-posed nature, the same mechanical responses in the physiological range can be achieved though the parameters are somewhat different. The dilemma in the in vivo inverse problem is that fewer data makes the inverse problem more ill-posed, but more measurements not only bring in extra uncertainties but also make the experiments challenging or inapplicable in vivo. By using a Bayesian statistical approach, we recently found that a and b in the HO law are identifiable, a_f is weakly identifiable, but not for other parameters if only using circumferential strains and the cavity volume. We are currently investigating which extra measurements (i.e. radial strain, shear strain, etc.) are needed in order to identify all parameters of the HO law through a global sensitivity study and uncertainty quantification. A further limitation in the HO law is that it does not take into account collagen fibre dispersion thought it can fit the experimental data very well [11], while a complex constitutive model will further complicate the identifiability issue of the inverse problem.

6 Conclusion

Studies on the constitutive modelling of soft tissues are critical for understanding the complex mechanobiology and pathogonesis, i.e. tumour progression and heart disease. In this study, the invariant-based fibre-reinforced strain energy function is introduced first within the continuum mechanics. The myocardium is then used as an example to demonstrate how to determine unknown material parameters from limited ex vivo experimental data, and later from in vivo measurements, which still remains a great challenge in the biomechanics community. The significant differences between the ex vivo and in vivo material property suggest that future studies are needed to bridge the gap from ex vivo to in vivo by taking into account inherent spatial heterogeneity and hierarchical microstructures, and the active growth and remodelling in biological tissue.

Acknowledgements We are grateful for the funding provided by the UK EPSRC (EP/N014642/1, EP/S030875, EP/S020950/1, EP/S014284/1). H.G. further acknowledges the EPSRC ECR Capital Award (308011). DG acknowledges funding from the Chinese Scholarship Council and the fee waiver from the University of Glasgow.

References

1. D Ambrosi and Francesco Mollica. On the mechanics of a growing tumor. *International journal of engineering science*, 40(12):1297–1316, 2002.
2. Mark Andrew Joseph Chaplain and Brian D Sleeman. Modelling the growth of solid tumours and incorporating a method for their classification using nonlinear elasticity theory. *Journal of mathematical biology*, 31(5):431–473, 1993.
3. Thierry Colin, Guillaume Dechristé, Jérôme Fehrenbach, Ludivine Guillaume, Valérie Lobjois, and Clair Poignard. Experimental estimation of stored stress within spherical microtissues. *Journal of mathematical biology*, 77(4):1073–1092, 2018.
4. Socrates Dokos, Bruce H Smaill, Alistair A Young, and Ian J LeGrice. Shear properties of passive ventricular myocardium. *American Journal of Physiology-Heart and Circulatory Physiology*, 283(6):H2650–H2659, 2002.
5. Thomas SE Eriksson, Anton J Prassl, Gernot Plank, and Gerhard A Holzapfel. Modeling the dispersion in electromechanically coupled myocardium. *International journal for numerical methods in biomedical engineering*, 29(11):1267–1284, 2013.
6. Min Fang, Jingping Yuan, Chunwei Peng, and Yan Li. Collagen as a double-edged sword in tumor progression. *Tumor Biology*, 35(4):2871–2882, 2014.
7. Daniel Fovargue, Marco Fiorito, Adela Capilnasiu, David Nordsletten, Jack Lee, and Ralph Sinkus. Towards noninvasive estimation of tumour pressure by utilising mr elastography and nonlinear biomechanical models: A simulation and phantom study. *Scientific reports*, 10(1):1–13, 2020.
8. H. Gao, W. G. Li, L. Cai, C. Berry, and X. Y. Luo. Parameter estimation in a Holzapfel–Ogden law for healthy myocardium. *Journal of Engineering Mathematics*, 95(1):231–248, December 2015.
9. Hao Gao, Andrej Aderhold, Kenneth Mangion, Xiaoyu Luo, Dirk Husmeier, and Colin Berry. Changes and classification in myocardial contractile function in the left ventricle following acute myocardial infarction. *Journal of The Royal Society Interface*, 14(132):20170203, 2017.
10. Debao Guan, Faizen Ahmad, Peter Theobald, Shwe Soe, Xiaoyu Luo, and Hao Gao. On the aic based model reduction for the general holzapfel-ogden myocardial constitutive law. *Biomechanics and Modeling in Mechanobiology*, 18:1213–1232, 2019.
11. Debao Guan, Jiang Yao, Xiaoyu Luo, and Hao Gao. Effect of myofibre architecture on ventricular pump function by using a neonatal porcine heart model: from dt-mri to rule-based methods. *Royal Society Open Science*, 7(4):191655, 2020.
12. Gerhard A. Holzapfel and Ray W. Ogden. Constitutive modelling of passive myocardium: a structurally based framework for material characterization. *Philosophical Transactions of the Royal Society A: Mathematical, Physical and Engineering Sciences*, 367(1902):3445–3475, September 2009.
13. Kenneth Hoyt, Benjamin Castaneda, Man Zhang, Priya Nigwekar, P Anthony di Sant'Agnese, Jean V Joseph, John Strang, Deborah J Rubens, and Kevin J Parker. Tissue elasticity properties as biomarkers for prostate cancer. *Cancer Biomarkers*, 4(4-5):213–225, 2008.
14. Stefan Klotz, Ilan Hay, Marc L Dickstein, Geng-Hua Yi, Jie Wang, Mathew S Maurer, David A Kass, and Daniel Burkhoff. Single-beat estimation of end-diastolic pressure-volume relationship: a novel method with potential for noninvasive application. *American Journal of Physiology-Heart and Circulatory Physiology*, 291(1):H403–H412, 2006.
15. Stelios K Kyriacou and Christos Davatzikos. A biomechanical model of soft tissue deformation, with applications to non-rigid registration of brain images with tumor pathology. In *International Conference on Medical Image Computing and Computer-Assisted Intervention*, pages 531–538. Springer, 1998.
16. Wenguang Li, Hao Gao, Kenneth Mangion, Colin Berry, and Xiaoyu Luo. Apparent growth tensor of left ventricular post myocardial infarction – in human first natural history study. *Computers in Biology and Medicine*, 129:104168, 2021.
17. Kenneth Mangion, Hao Gao, Dirk Husmeier, Xiaoyu Luo, and Colin Berry. Advances in computational modelling for personalised medicine after myocardial infarction. *Heart*, 104(7):550–557, 2018.

18. Andrey V Melnik, Xiaoyu Luo, and Ray W Ogden. A generalised structure tensor model for the mixed invariant I8. *International Journal of Non-Linear Mechanics*, September 2018.
19. Joseph J O'Hagan and Abbas Samani. Measurement of the hyperelastic properties of tissue slices with tumour inclusion. *Physics in Medicine & Biology*, 53(24):7087, 2008.
20. Gerhard Sommer, Andreas J Schriefl, Michaela Andrä, Michael Sacherer, Christian Viertler, Heimo Wolinski, and Gerhard A Holzapfel. Biomechanical properties and microstructure of human ventricular myocardium. *Acta biomaterialia*, 24:172–192, 2015.
21. Triantafyllos Stylianopoulos. The solid mechanics of cancer and strategies for improved therapy. *Journal of biomechanical engineering*, 139(2), 2017.
22. Peter A Torzilli, Jonathan W Bourne, Tessa Cigler, and C Theresa Vincent. A new paradigm for mechanobiological mechanisms in tumor metastasis. In *Seminars in Cancer Biology*, volume 22, pages 385–395. Elsevier, 2012.
23. GU Unnikrishnan, VU Unnikrishnan, JN Reddy, and CT Lim. Review on the constitutive models of tumor tissue for computational analysis. *Applied Mechanics Reviews*, 63(4), 2010.
24. Chrysovalantis Voutouri, Fotios Mpekris, Panagiotis Papageorgis, Andreani D Odysseos, and Triantafyllos Stylianopoulos. Role of constitutive behavior and tumor-host mechanical interactions in the state of stress and growth of solid tumors. *PloS one*, 9(8):e104717, 2014.
25. HM Wang, H Gao, XY Luo, C Berry, BE Griffith, RW Ogden, and TJ Wang. Structure-based finite strain modelling of the human left ventricle in diastole. *International journal for numerical methods in biomedical engineering*, 29(1):83–103, 2013.
26. Shuaishuai Xu, Huaxiang Xu, Wenquan Wang, Shuo Li, Hao Li, Tianjiao Li, Wuhu Zhang, Xianjun Yu, and Liang Liu. The role of collagen in cancer: from bench to bedside. *Journal of translational medicine*, 17(1):1–22, 2019.